Pictures and tables to be inserted in the Final Report

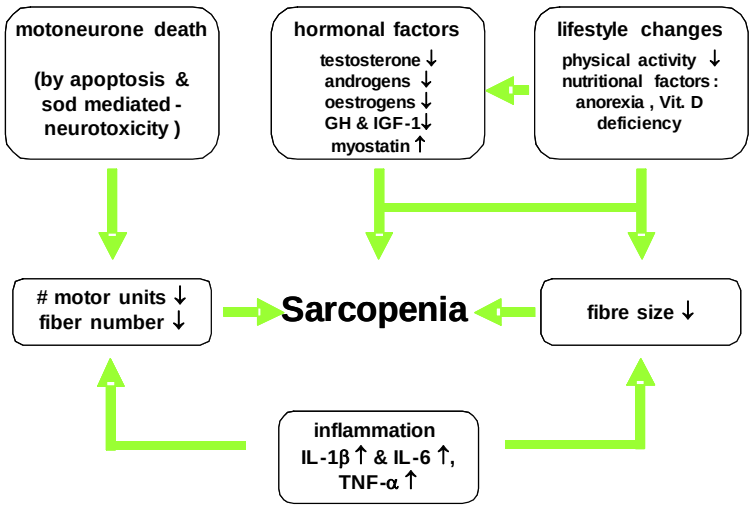

Figure 1: scheme of the multifactorial process leading to sarcopenia

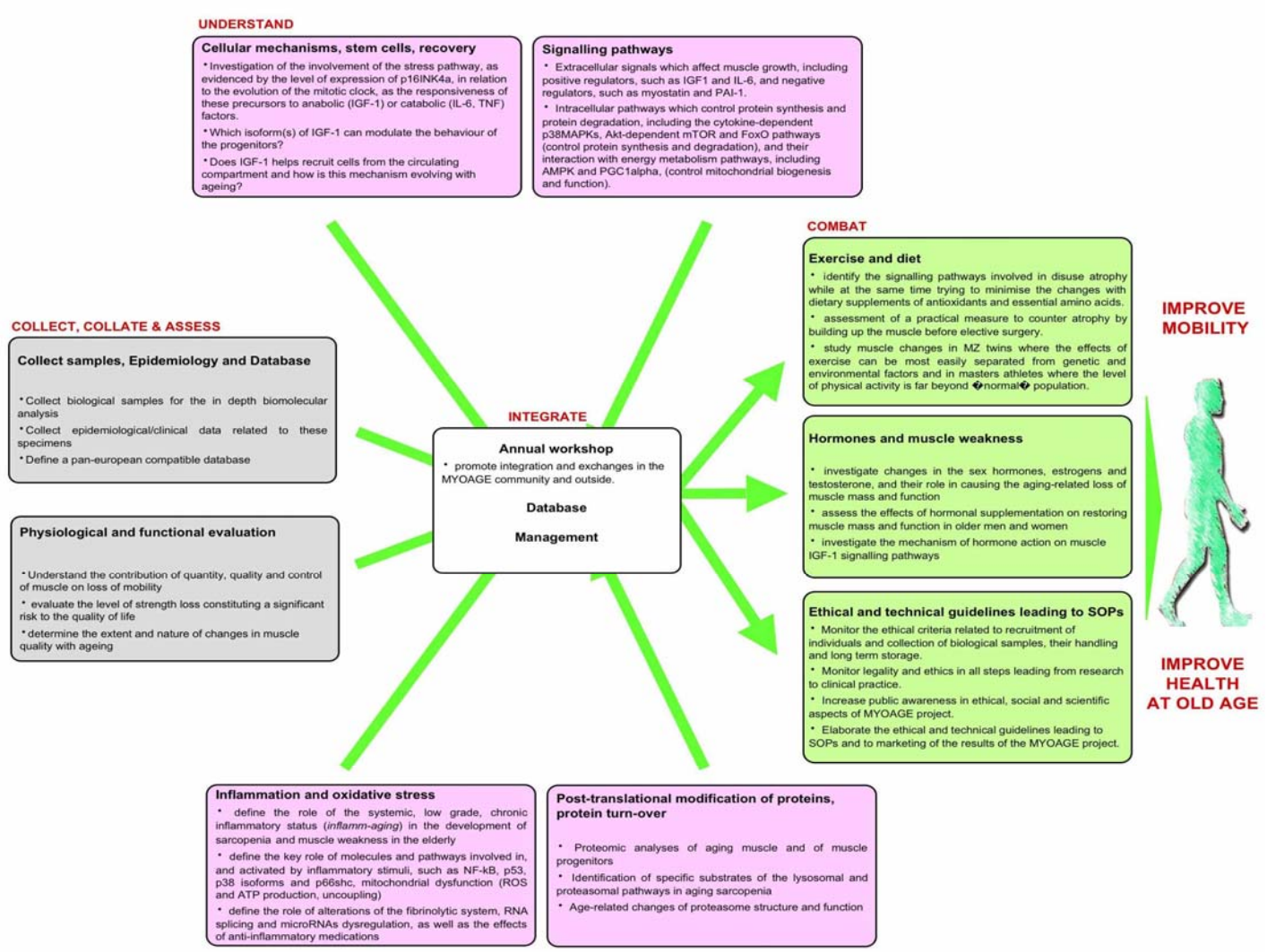

Figure 2: illustration of the MYOAGE strategy

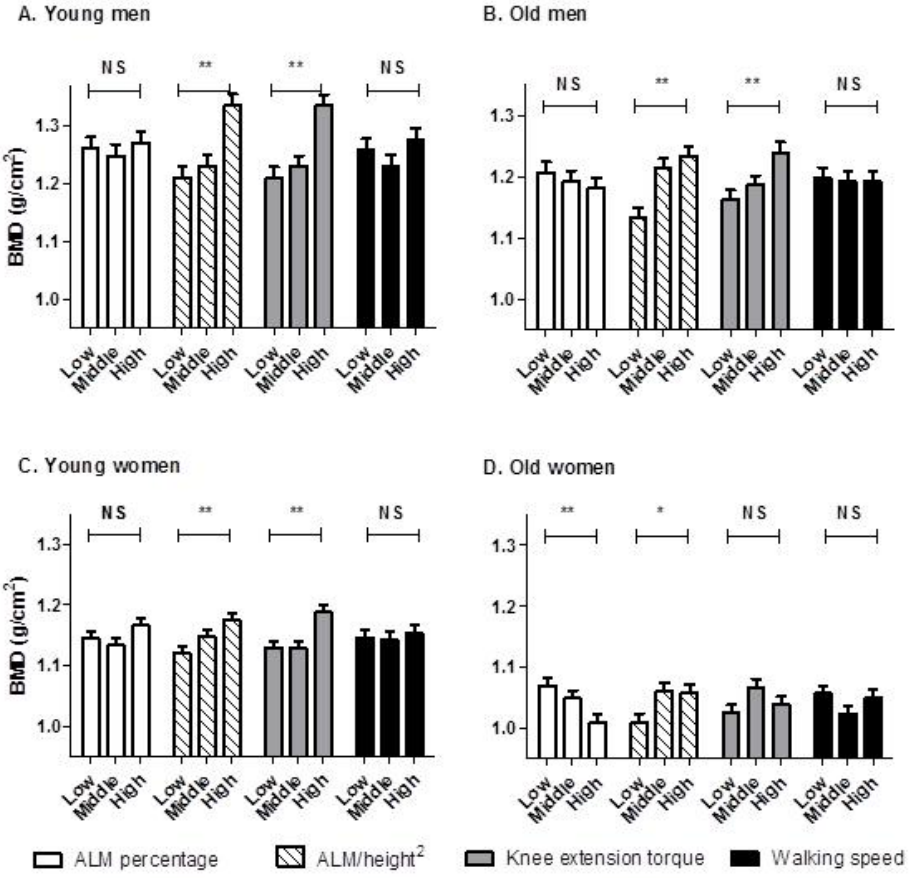

Figure 2.1. The association between different diagnostic criteria of sarcopenia and whole body bone mineral density (BMD) in young men (a), old men (b), young women (c) and old women (d). ALM in percentage is the appendicular lean mass as percentage of body mass. ALM percentage, ALM/height^2 (kg/m^2), knee extension torque (Nm) and walking speed (m/s) are presented in country, sex, and age group specific tertiles. Bars represent the adjusted means and s.e. *P* values were calculated with linear regression models with adjustments for age and country. *=p<0.01. **=p<0.001.

	Young (n=182)	Old (n=322)	P-value
Age (years)	23.4 (2.9)	74.4 (3.3)	**<0.0005**
Females, n (%)	96 (52.7)	161 (50.0)	0.554
Living with partner, n (%)[a]	40 (26.8)	173 (64.8)	**<0.0005**
Highly educated, n (%)[b]	134 (87.6)	119 (44.6)	**<0.0005**
Anthropometry			
Height (m)	1.73 (0.09)	1.67 (0.09)	**<0.0005**
Body mass (kg)	68.7 (12.3)	71.6 (12.7)	**0.014**
Body mass index ($kg \cdot m^2$)	22.8 (3.0)	25.6 (3.3)	**<0.0005**
Lifestyle			
High alcohol use [c], n (%)	22 (12.1)	28 (8.7)	0.221
Current smoking, n (%)	24 (13.2)	14 (4.3)	**<0.0005**
Comorbidities			
Number of diseases, median (IQR)	0 (0-0)	1 (0-1)	**<0.0005**
Number of medications, median (IQR)	0 (0-1)	1 (0-3)	**<0.0005**
Mental state			
MMSE score (points), median (IQR)	30 (29-30)	29 (28-30)	**<0.0005**
GDS score (points), median (IQR)[d]	0 (0-1)	1 (0-2)	**<0.0005**
Diagnostic criteria for sarcopenia			
Lean mass percentage (%) [e]	72.8 (9.1)	66.6 (8.3)	**<0.0005**
ALM percentage (%) [f]	33.1 (4.7)	28.6 (4.1)	**<0.0005**
ALM/height² (kg/m^2)	7.5 (1.3)	7.2 (1.1)	**0.013**
Total lean mass (kg)	50.1 (11.4)	47.4 (9.9)	**0.008**
Knee extension torque (Nm) [g]	196.6 (69.6)	126.5 (46.0)	**<0.0005**
Handgrip strength (Kg) [g]	42.3 (12.3)	33.1 (9.6)	**<0.0005**
Physical performance			
TUG (s) [h]	4.85 (0.91)	6.24 (1.16)	**<0.0005**
Walking speed (m/s)	1.85 (0.30)	1.49 (0.23)	**<0.0005**
One-leg balance with eyes open (sec), median (IQR) [g]	30.0 (30-30)	30.0 (15-30)	**<0.0005**
One-leg balance with eyes closed (sec), median (IQR) [g]	30.0 (20-30)	4.0 (2-6)	**<0.0005**

Variables are presented as mean (standard deviation), unless indicated otherwise. For strength and performance measurements the best effort has been used for analysis. Independent samples t-tests were used to assess differences between young and old. [a] Data available in n=416. [b] Data available in n=420. [c] High alcohol use defined as for males > 21 units/week and females > 14 units/week. [d] Data available in n=411. [e] Total lean mass as percentage of total body mass. [f] ALM (appendicular lean mass) as percentage of total body mass. [g] The highest value from the duplicate measurements has been used for analysis. [g] The fastest time from the duplicate measurements has been used for analysis. MMSE: mini mental state examination. GDS: geriatric depression scale. TUG: Timed Up and Go test.

Table 2.1: Participant characteristics, stratified by age (n=504).

		ALM	ALM/ht2	Q Vol	Q:Bone	MVC	MVC/BM	Power	Power/BM
YF	6MWD	0.034	0	0.007	0.018	0.003	0.011	0.139	0.004
	TUG	0.024	0.011	0.206	0.003	0.156	0.012	0.073	0.116
OF	6MWD	0.039	0.029	0.122	0.021	0.134	0.128	0.221	0.409
	TUG	0.017	0	0.078	0.026	0.081	0.088	0.179	0.338
YM	6MWD	0.035	0.0237	0.04	0.001	0	0.034	0.01	0.025
	TUG	0.01	0.011	0.313	0.109	0.131	0.076	0	0.022
OM	6MWD	0.118	0.052	0.009	0.003	0	0.055	0.057	0.284
	TUG	0.122	0.177	0.002	0.001	0.083	0.001	0.195	0.097

Young female (YF); old female (OF); young male (YM); old male (OM). Significant relationships shown in red text.

Table 2.2. Mobility in relation to muscle size and function.

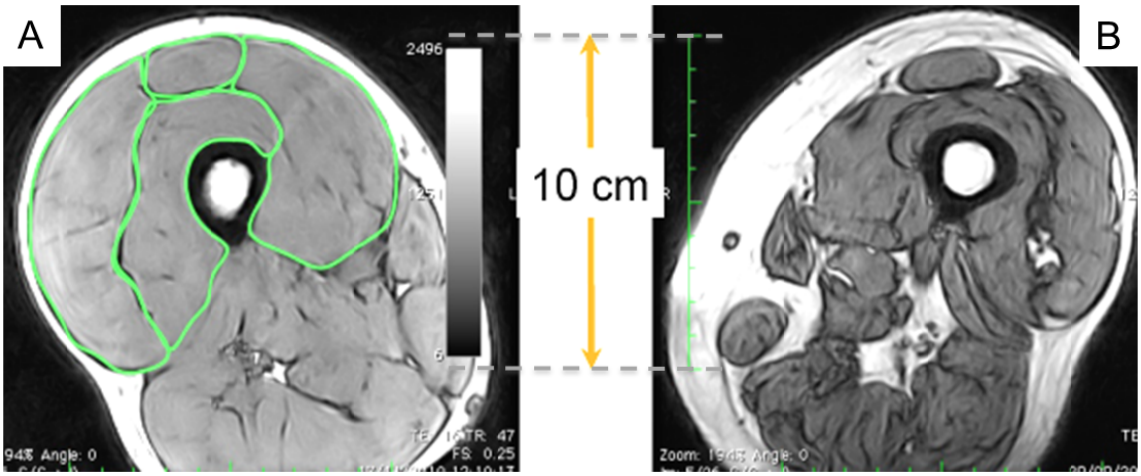

Figure 2.2. Magnetic resonance images of the mid-thigh. *A young man is shown in A (age 24 yrs, with quadriceps muscles highlighted), an older man is shown in B (aged 80 yrs). All muscles were visibly smaller in the thigh of the older man, and also typical of ageing is the increased adipose tissue.*

Modified from McPhee et al 2013., Biogerontology

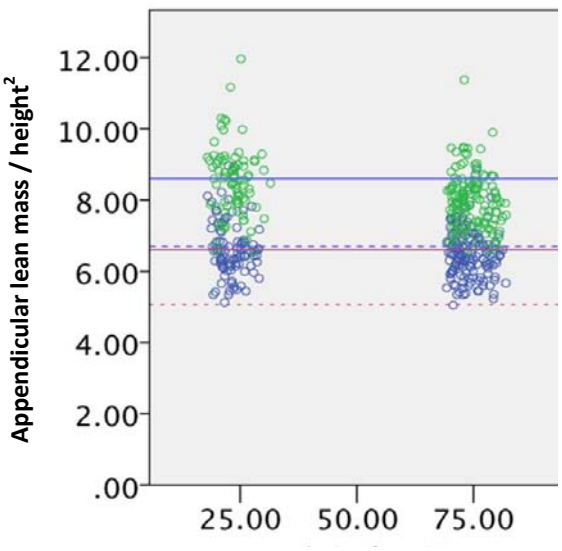

Figure 2.3A. Appendicular lean mass measured using DXA and normalised to height^2 to estimate the prevalence of *sarcopenia* in the MYOAGE cohort.

The green line represents men and the red line women. The solid lines are the mean and the dashed lines are 2 standard deviations below the mean of the young.

Only 5% of older participants were below the dashed line and classified as sarcopenic

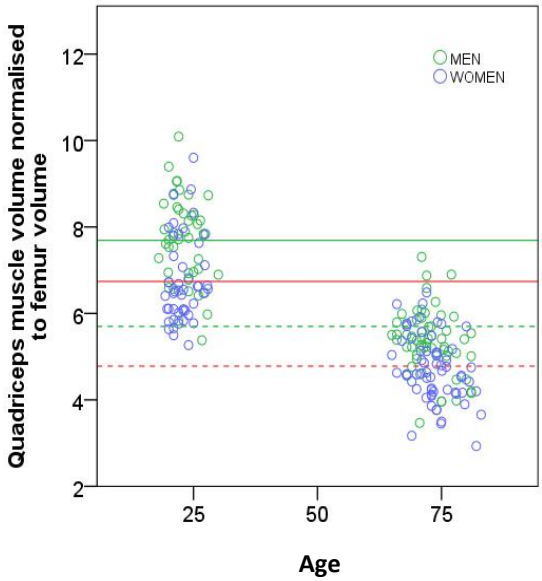

Figure 2.3B. Quadriceps muscle volume measured using MRI and normalised to femur volume to estimate the prevalence of *sarcopenia* in the MYOAGE cohort.

The green line represents men and the red line women. The solid lines are the mean and the dashed lines are 2 standard deviations below the mean of the young.

74% of older men and 58% of older women were below the dashed lines and classified as sarcopenic.

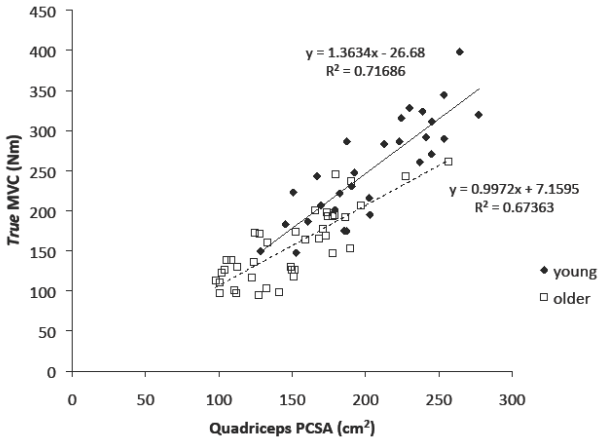

Figure 2.4A. Maximal voluntary contraction (MVC) is strongly related to quadriceps physiological cross sectional area (PCSA). Older people were weaker than would be expected from their muscle size.

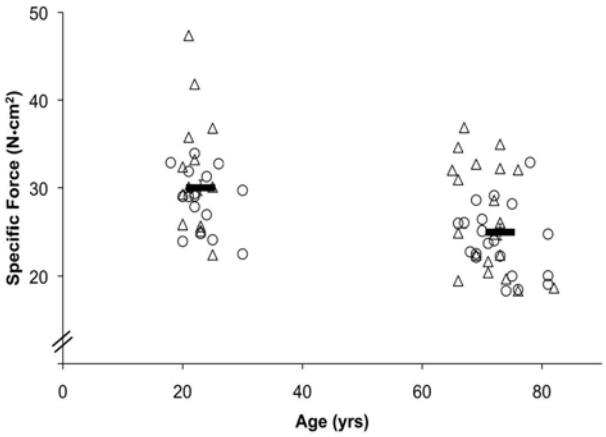

Figure 2.4B. Specific force of quadriceps muscles was 16.5% lower in old compared with young. Triangles are women and circles, men. Bold horizontal lines indicate mean for young and old.

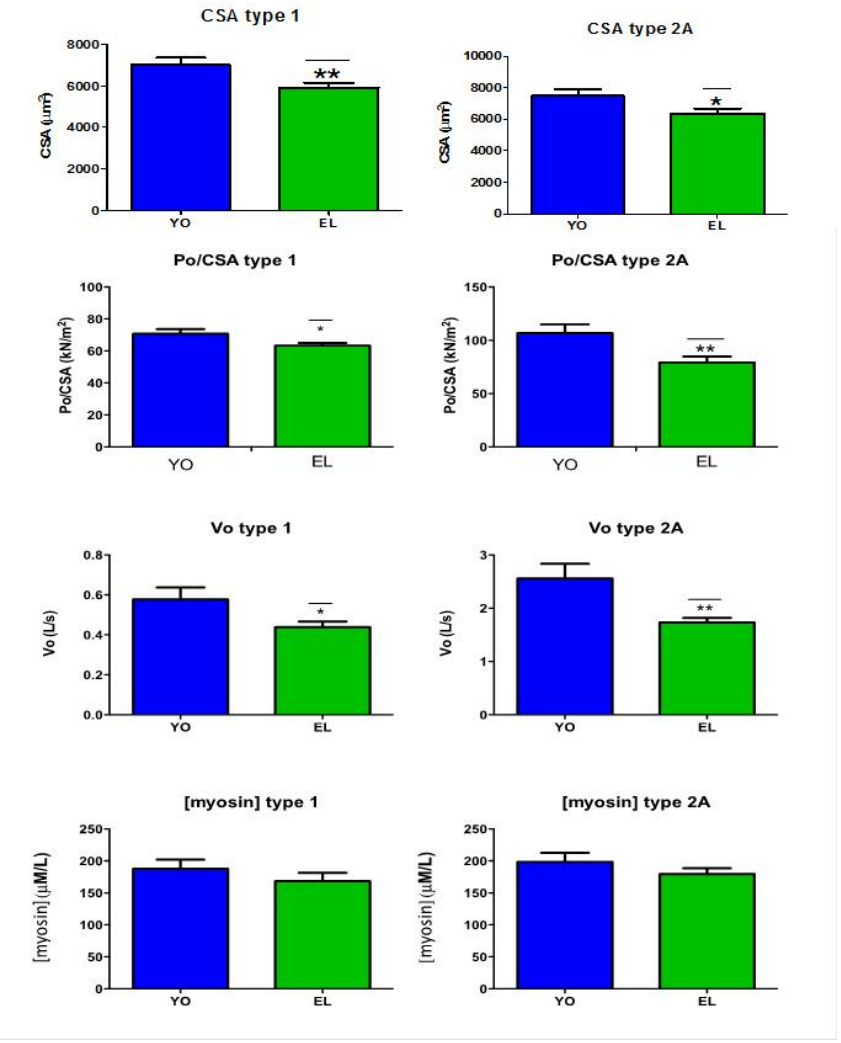

Figure 2.5. Analysis of isolated muscle fibres. Older muscle had lower fibre cross sectional area (csa) in type 1 and 2 fibres, lower specific tension (Po/csa) and lower velocity of shortening (Vo). Myosin concentration did not differ between young and old.

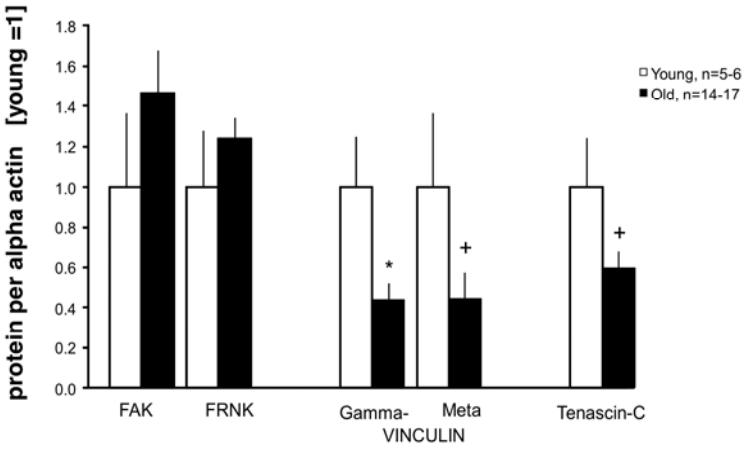

Figure 2.6. Costameric proteins in young and older muscles. *Cross indicates significant difference between groups.*

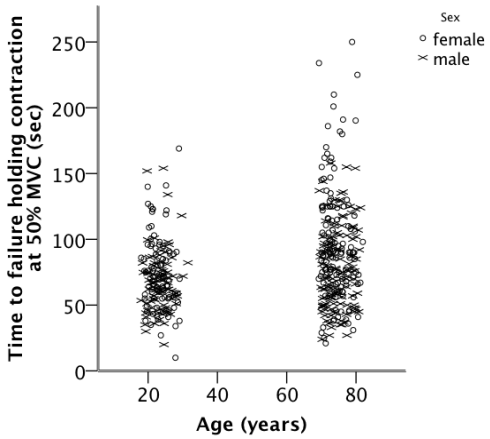

Figure 2.7. Older people held a sustained isometric knee extension for longer than young. *There was very large variability between people*

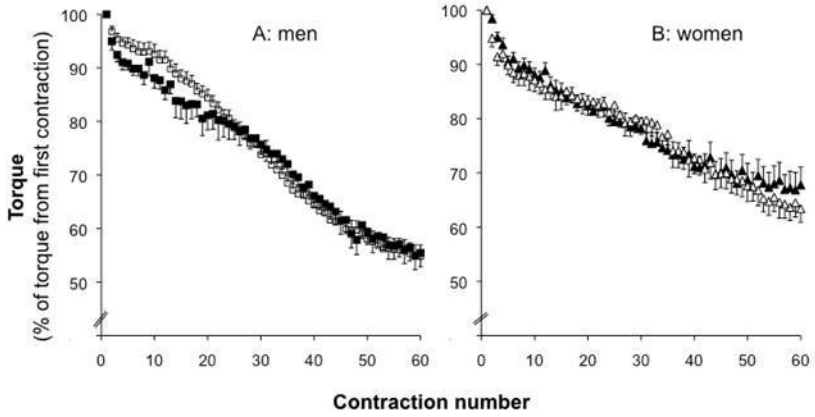

Figure 2.8. Older and young people showed similar fatigue after 60 brief intermittent contractions. *Women fatigued less than men.*

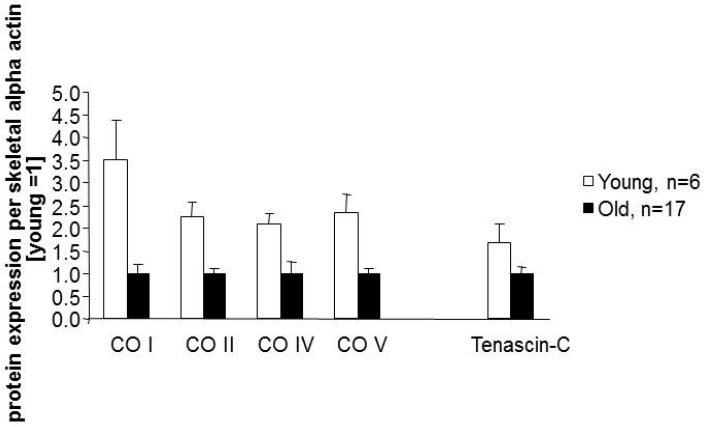

Figure 2.9. Older people had lower levels of mitochondrial proteins compared with young.

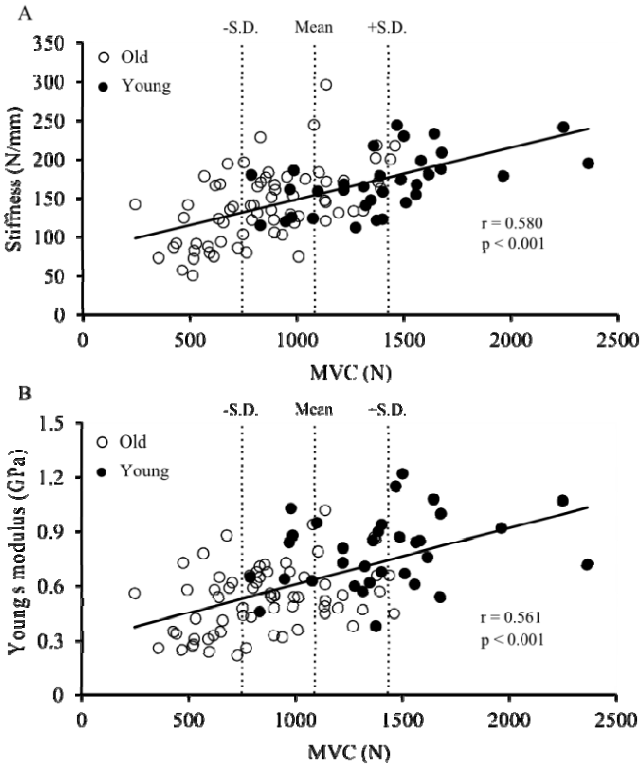

Figure 2.10. Achilles tendon and young's modulus were lower in old compared with young.

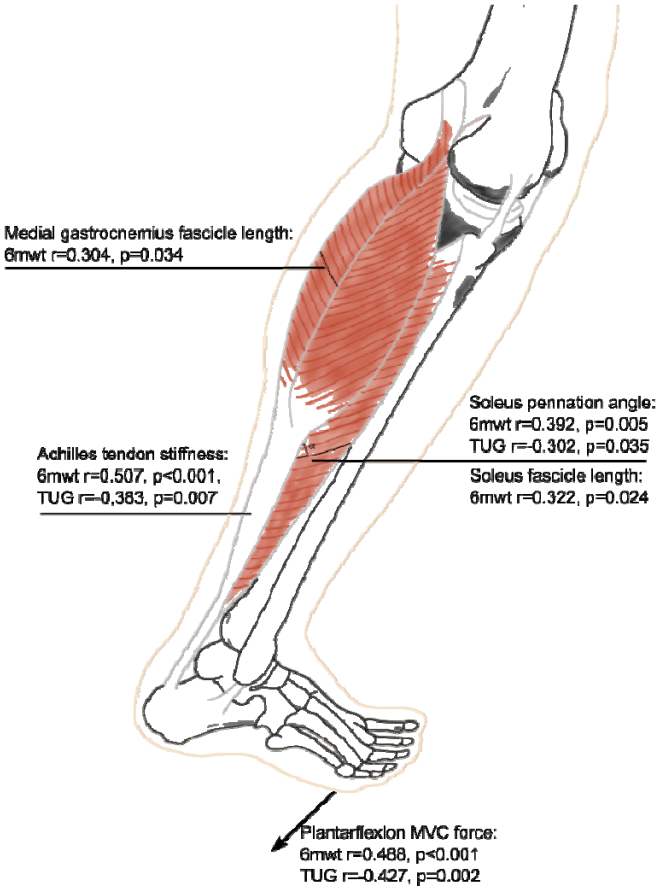

Figure 2.11. Association between characteristics of the lower leg and mobility.

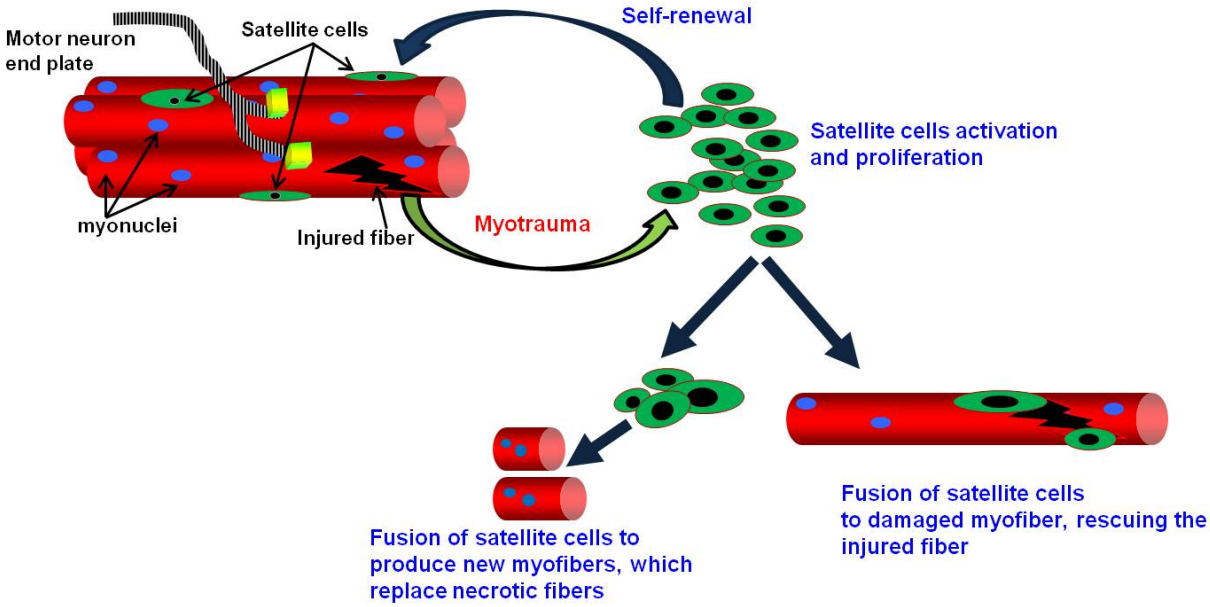

Figure 3.1 Model of satellite cells-mediated muscle regeneration

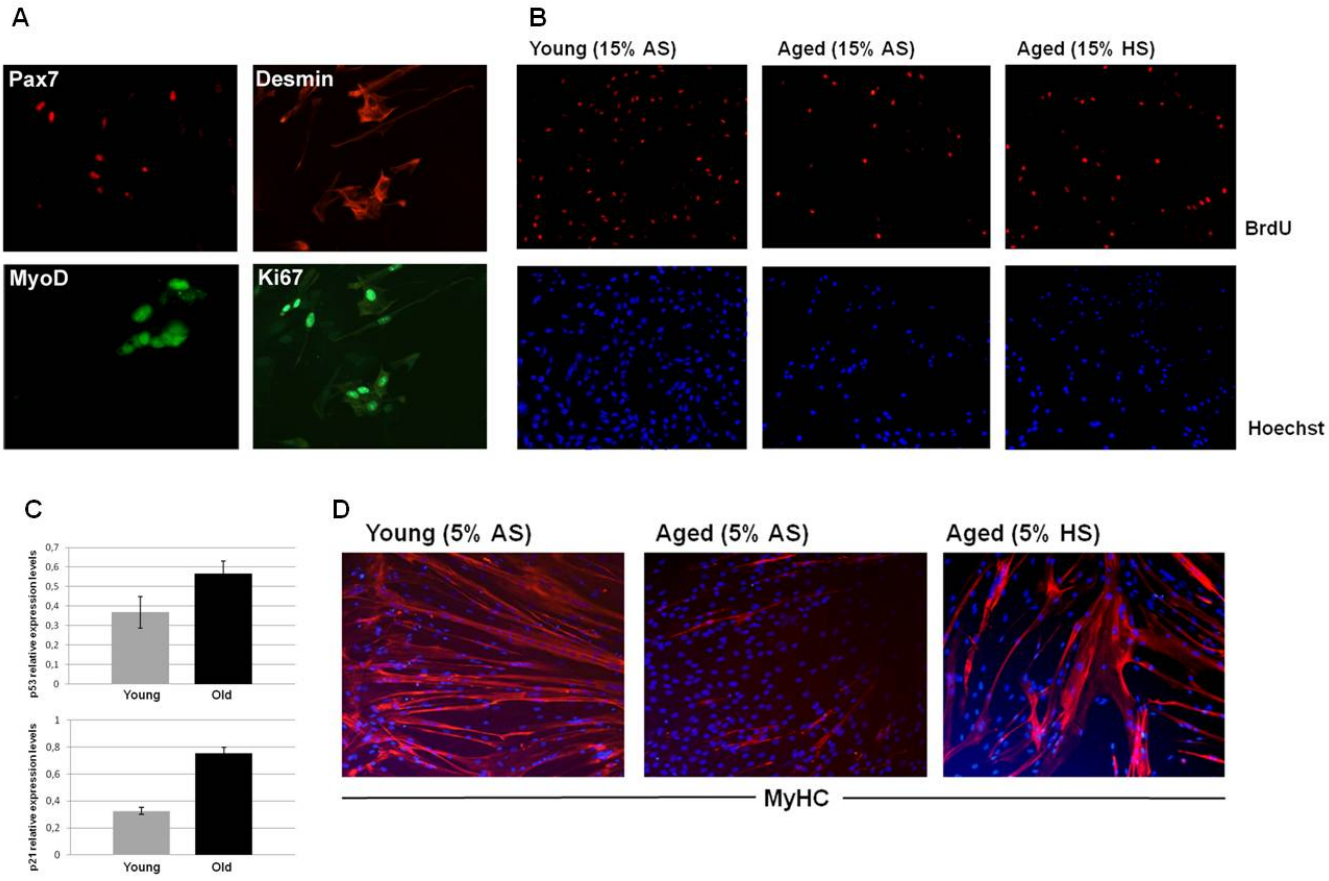

Figure 3.2 *Aged satellite cells although are able to proliferate (A), display a delayed response to activating stimuli and a reduced proliferative response to their sub-optimal environment (B), which might be caused by the altered expression/activity of p53 pathway (C) and display a defect in muscle differentiation when cultured in autologous serum (D).*

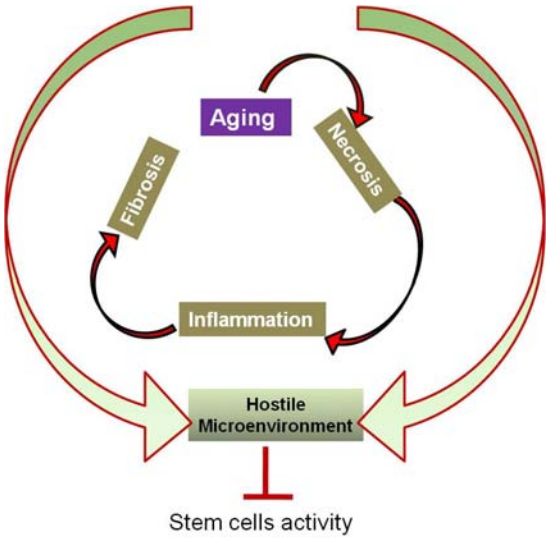

Figure 3.3. *Schematic representation of pathologic alterations associated with aging, which create an hostile microenvironment that in turn affects the activity of stem cells.*

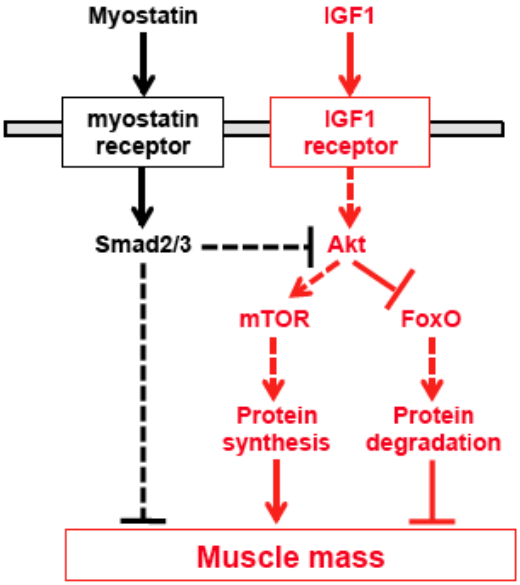

Figure 4.1. Scheme of the two major pathways involved in muscle mass regulation, based on the knowledge available when the MYOAGE project started in 2009.

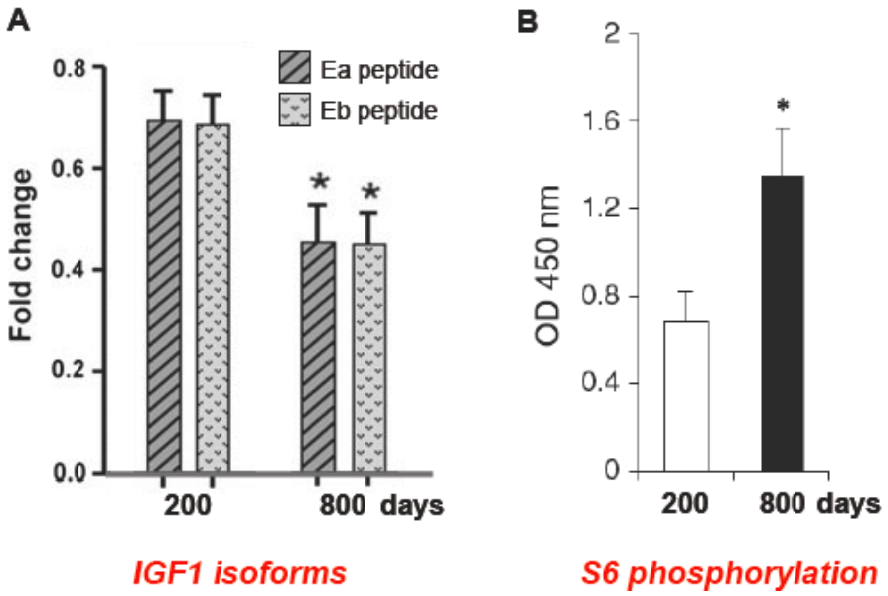

Figure 4.2. IGF1 isoform distribution and S6 phosphorylation differ in skeletal muscle from very old (800-day-old) mice compared to adult (200-day-old) animals. (A) Skeletal muscles from very old mice show a difference in IGF-1 isoform expression, with significant reduction in Ea and Eb C-terminal E peptides. (B) Increased S6 phosphorylation in muscles from very old mice points to increased mTOR-S6K activity during ageing. (Sandri et al, Biogerontology 2013).

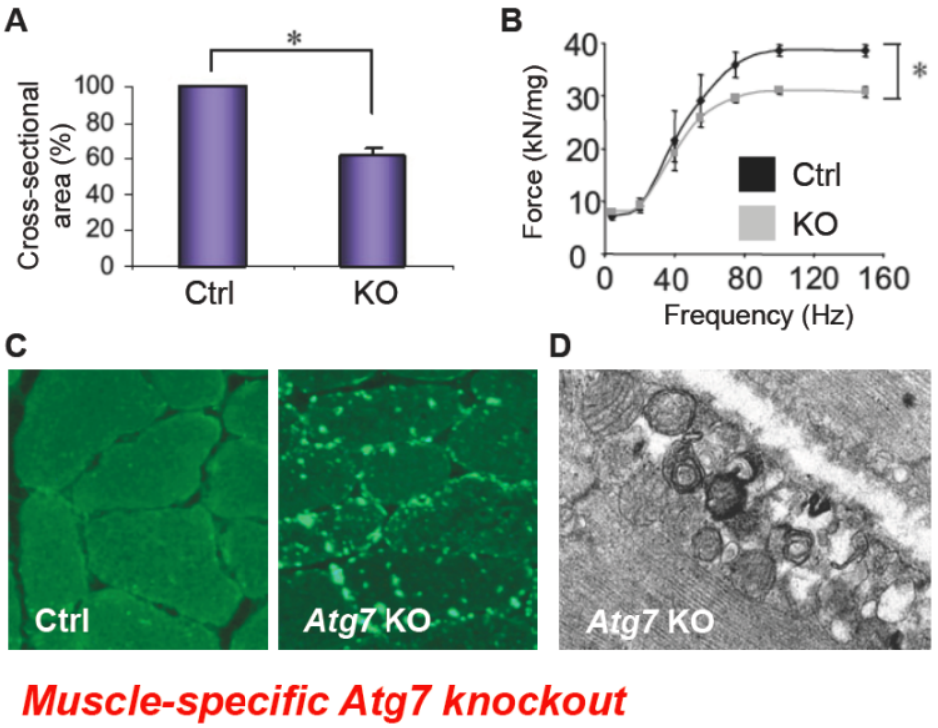

Figure 4.3. Muscle-specific knockout of the autophagy gene, *Atg7*, causes muscle atrophy (A), reduced muscle force (B), accumulation of protein aggregates visualized by p62 immunofluorescence (C), and accumulation of abnormal mitochondria with aberrant membranous structures visualized by electron microscopy (D). These findings indicate that the autophagy flux is important to preserve muscle mass and maintain myofibre integrity, whereas the inhibition of autophagy leads to myofibre degeneration and weakness (Masiero et al, Cell Metab 2009).

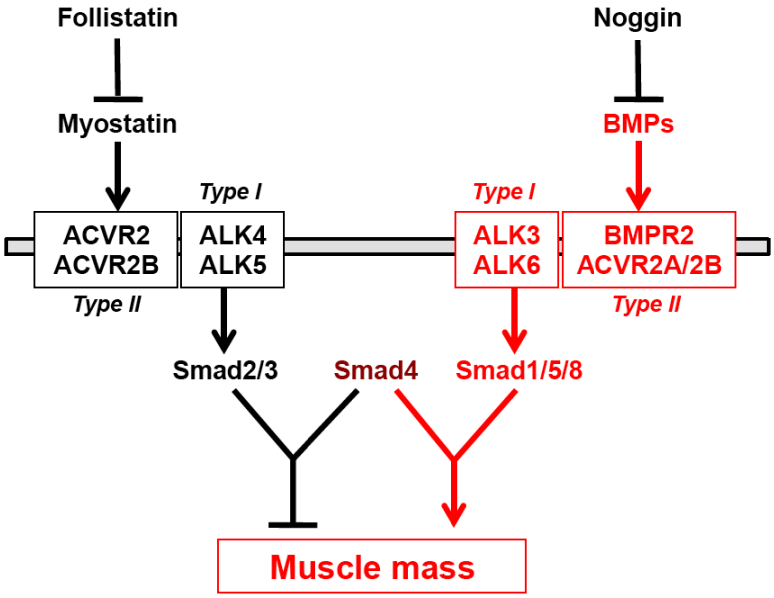

Figure 4.4. The scheme illustrates a novel concept in muscle growth regulation, which emerged during the last phase of activity of WP4. We found that muscle mass is controlled by the balance between myostatin signalling, acting as a negative regulator of muscle growth, and BMP signalling, acting as a positive regulator of muscle growth. Both myostatin and BMPs are TGF-β ligands and bind to type I receptors, such as activin receptor 2 (ACVR2) or bone morphogenetic protein receptor 2 (BMPR2), which in turn recruit type II receptors, such as ALK4 or ALK3. Active receptor complexes formed upon myostatin or BMP binding induce the phosphorylation of Smad 2/3 or Smad1/5/8, respectively. Phosphorylated Smad2/3 or Smad1/5/8 bind in turn to Smad4 and the heterodimers translocate to the nucleus and activate target genes, which differ between the two pathways and lead to opposite effects on muscle mass: activation of the myostatin pathway leads to muscle atrophy, while the activation of the BMP pathway leads to muscle hypertrophy. The analysis of these pathways is complicated by the existence of multiple ligands (myostatin-like factor, such as activin A, and multiple BMPs) and antagonistic factors (myostatin antagonists, such as follistatin, and BMP antagonists, such as noggin). (Sartori et al, Nature Genet, in press).

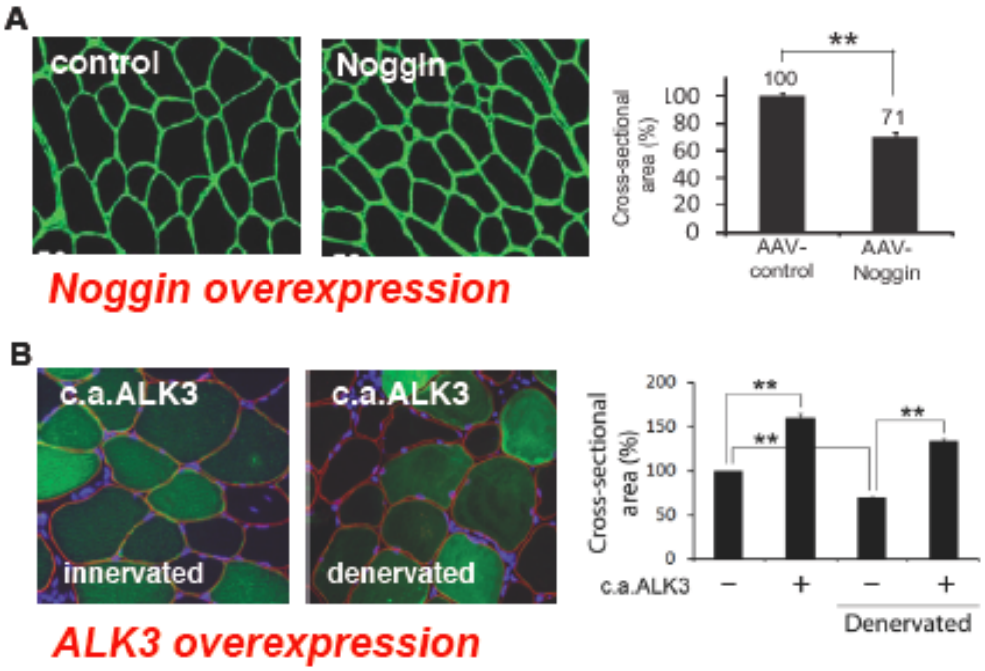

Figure 4.5. *A. Inhibition of the BMP pathway leads to muscle atrophy*. Muscles transfected with Noggin (BMP antagonist) show decreased myofibre size. *B. Activation of the BMP pathway induces muscle hypertrophy*. Intramuscular overexpression of a constitutively active type I BMP receptor (c.a.ALK3) leads to muscle hypertrophy in adult mouse muscles and prevents muscle atrophy after nerve section. (Sartori et al, Nature Genet, in press)

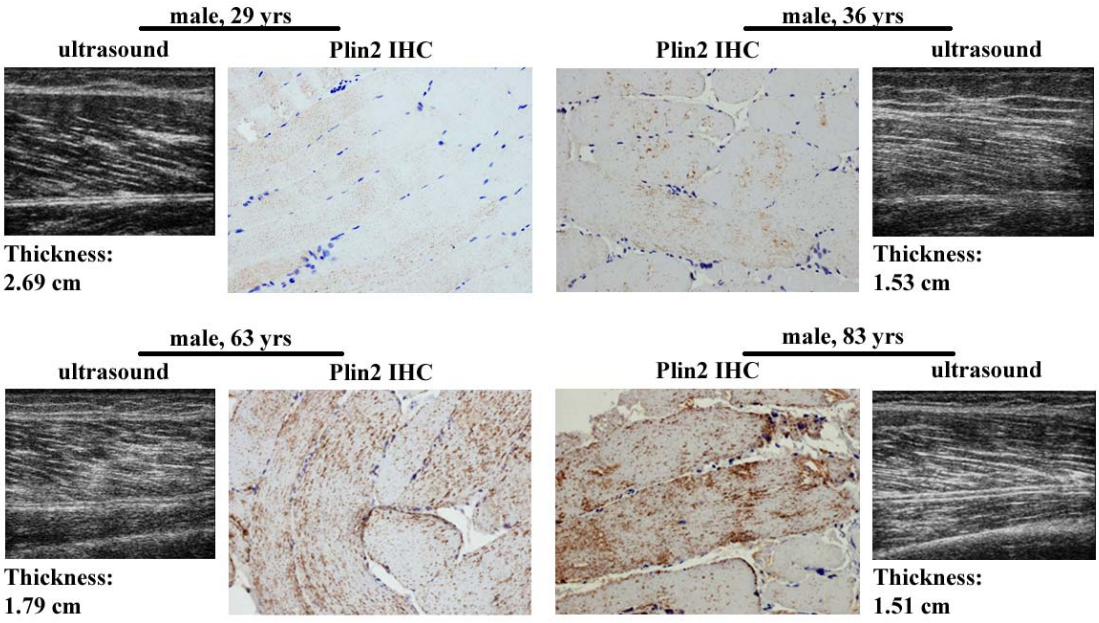

Figure 5.1. Representative example of the correlation between muscle thickness, measured by ultrasound analysis, and Plin2 expression (brown dots of Immuno histochemistry, IHC, images) in v. lateralis from young and old subjects.

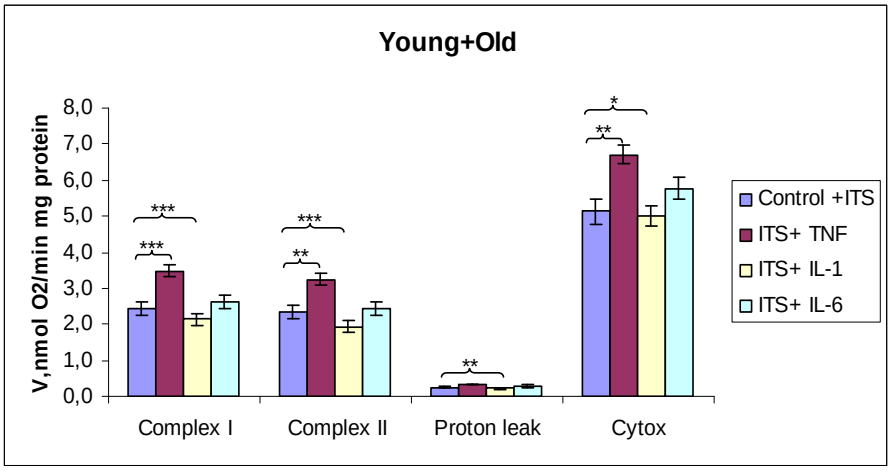

Figure 5.2. Comparison of the effects of TNF-α, IL-1β and IL-6 on respiratory parameters of the myogenic cells of the old and young persons cultured either in the presence of ITS (control, +ITS) or ITS and one of three cytokines. The respiratory parameters were normalized on protein.

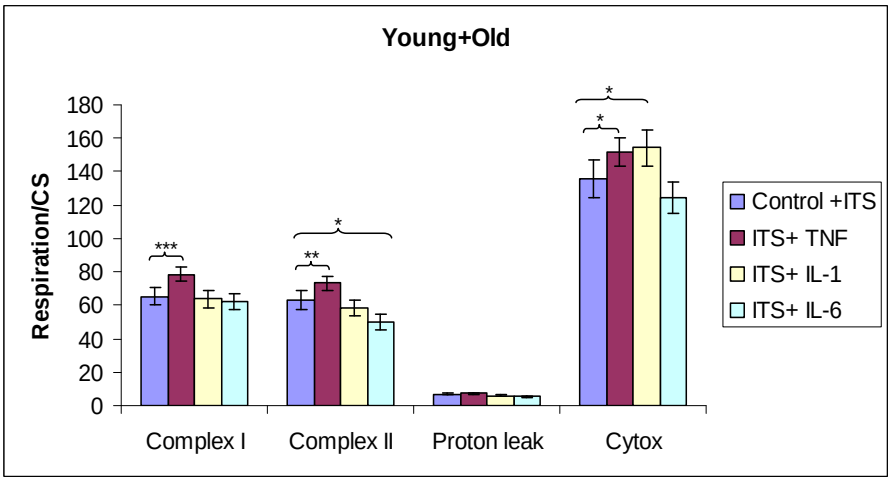

Figure 5.3. Comparison of the effects of TNF-α, IL-1β and IL-6 on respiratory parameters of the myogenic cells of the old and young persons cultured either in the presence of ITS (control, +ITS) or ITS and one of three cytokines. The respiratory parameters were normalized on the content of citrate synthase (CS).

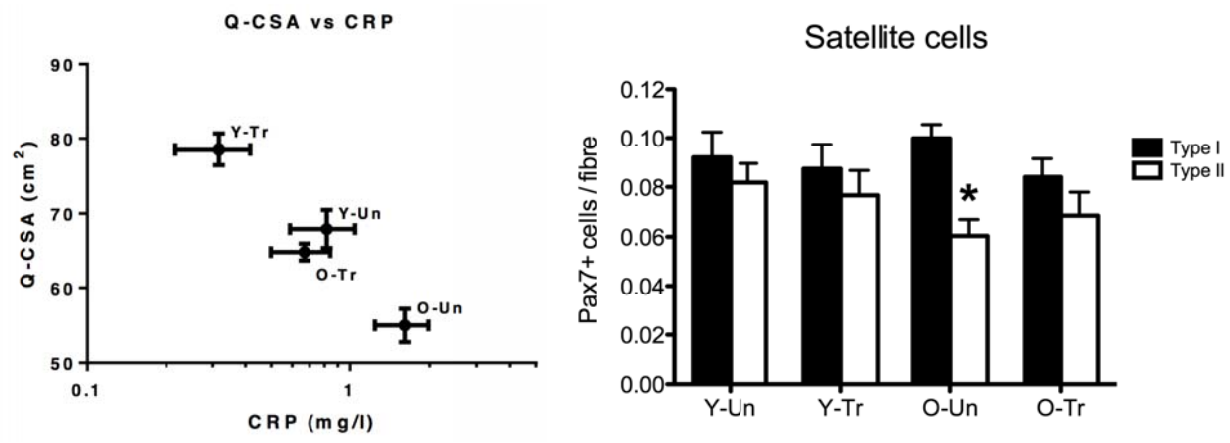

Figure 5.4.

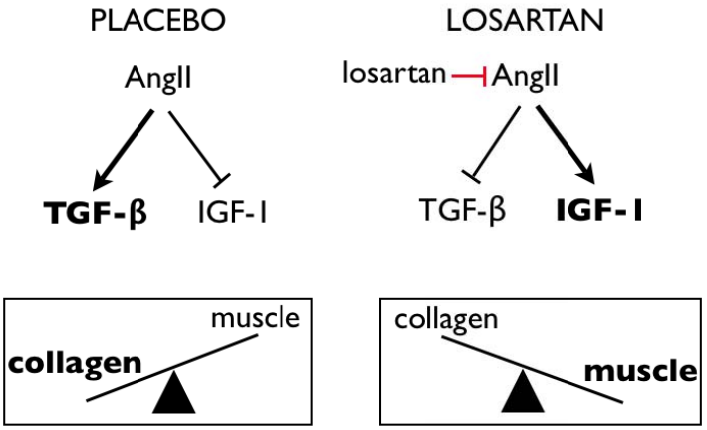

Figure 5.5. Hypothesised effect of Angiotensin II blocker on muscle.

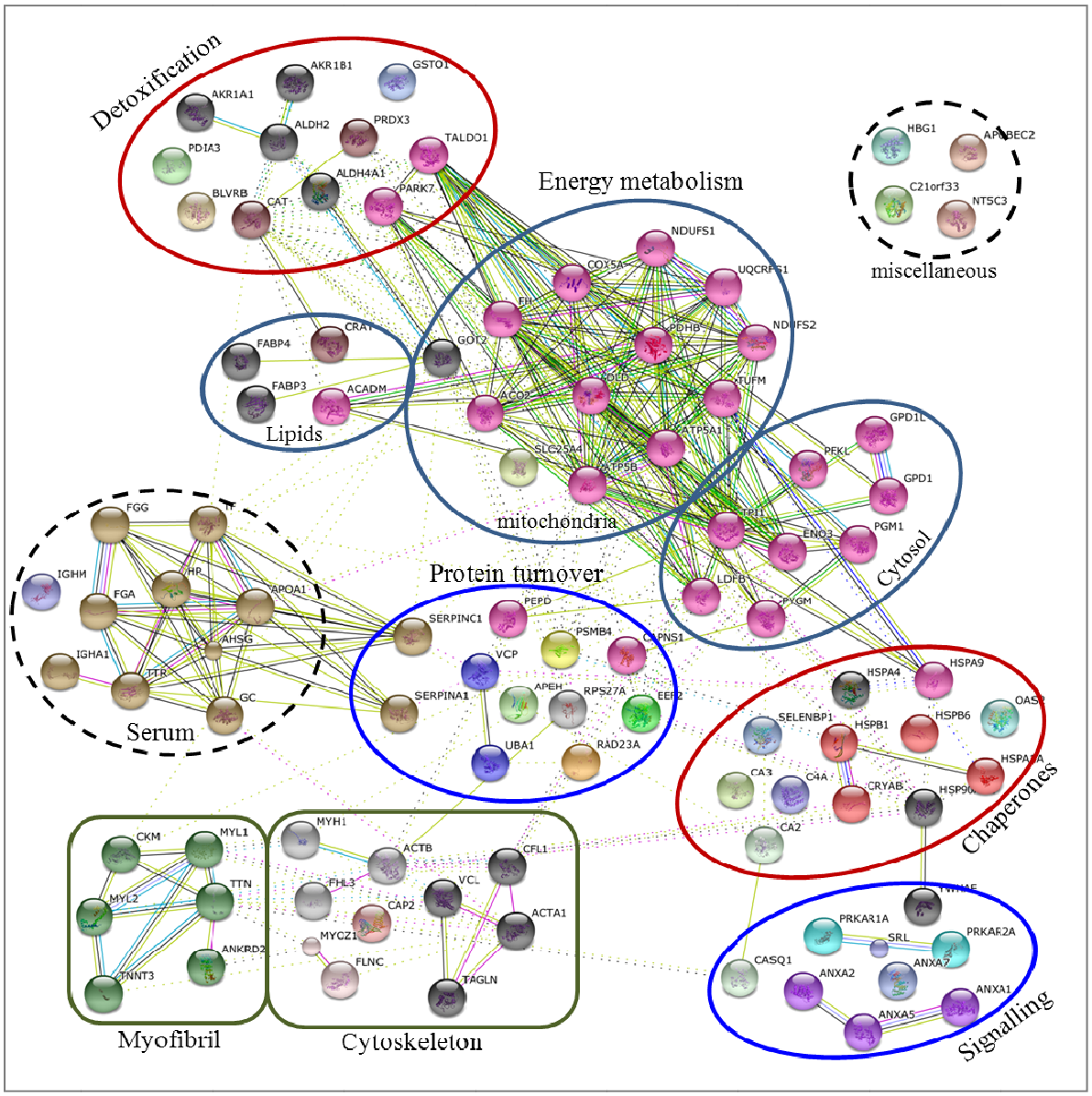

Figure 6.1. Data mining of the expression proteomics analysis

A)

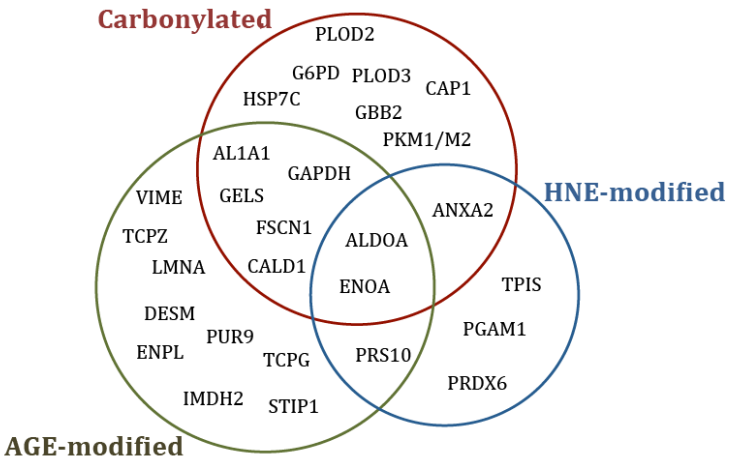

B)

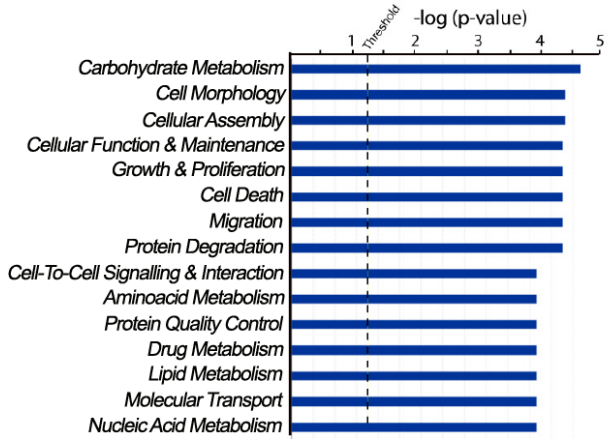

Figure 6.2. Identification and data mining of modified proteins. A) Venn diagram depicting the distribution of proteins in relation with the modifications studied. B) Modified proteins were grouped in functional categories through the use of Ingenuity Pathways Analysis. The bars represent the biological functions identified, named in the x-axis. The dotted line represents the threshold above which there are statistically significantly more proteins in a biological function than expected by chance.

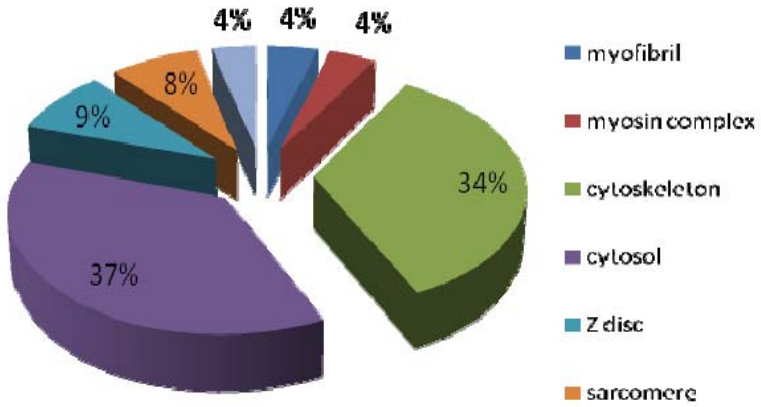

Figure 6.3. Anomalous protein accumulation in Atrogin-1 knock-out mice.SILAC-based proteomics showed anomalous accumulation of proteins from different cellular compartments in adult Atrogin-1 KO.

Figure 7.1 *The 1st on Tor, caloric restriction and anabolism in ageing periodic Workshop was organised in Split from September 22nd to 25th, 2010.*

Figure 7.2 *The 2nd periodic Workshop on Muscle Mass Regulation was organized in Acaya, near Lecce, Italy from September 23rd to 25th, 2011.*

Figure 7.3 *The 3rd periodic Workshop on Inflammation and ECM remodelling in Ageing was organised in Barcelona, Spain from December 1st to 2nd, 2011.*

Figure 7.4 *Last workshop in the serie, the 4th periodic Workshop entitled The aging human muscle: An integrated machinery was organised in Copenhagen, Denmark from August 30th to 31st, 2012.*

A 

B 

C 

D 

E 

Figure 7.5 *MYOAGE participation to the EMC meeting in Rhodes September 1st to 5th 2013*

A- *Prof. Stefano Schiaffino (VIMM) giving the opening keynote presentation to the EMC participants*

B- *Dr. Gillian Butler-Browne (Inserm) and Prof. Marco Narici (MMU) chairing the muscle aging session*

C-*Dr. Gillian Butler-Browne opening the ageing muscle session at the EMC*

D- *the MYOAGE WP leaders ready to answer the questions following their presentations. From left to right: Pr. Claudio Franceschi, Pr. Marco Sandri, Pr. Sarianna Sipilä, Pr. Roberto Bottinelli, Pr. Antonio Musaro and Pr. Bertrand Friguet.*

E- *Group photo of the EMC 2012 Participants including MYOAGE members.*

Table 1 Quadriceps MVC, voluntary activation capacity, PCSA and specific force and baseline, post-ULLS and post-RT. Data are mean ± SEM

	ULLS (n = 8)			Control (n=8)	
	Baseline	3 weeks post-ULLS	6 weeks post-RT	Pre	Post
MVC	299 ± 14	221 ± 14**	291 ± 14††	311 ± 21	294 ± 26
VA	87 ± 3.5	83 ± 3.5	88 ± 3	–	–
$EMG_{RMS/M\text{-}wave}$	0.073 ± 0.02	0.0614 ± 0.02	0.073 ± 0.02	0.070 ± 0.01	0.070 ± 0.01
PCSA	208 ± 6	203 ± 8	218 ± 14	199.98 ± 18.0	202.66 ± 21.7
SF	32 ± 2	24 ± 1*	35 ± 3†	38.0 ± 4.4	37.1 ± 6.3

* Significantly different from baseline; $p < 0.05$; ** significantly different from baseline $p < 0.005$; † significantly different from post-ULLS $p < 0.05$; †† significantly different from post-ULLS $p < 0.005$

Table 8.1

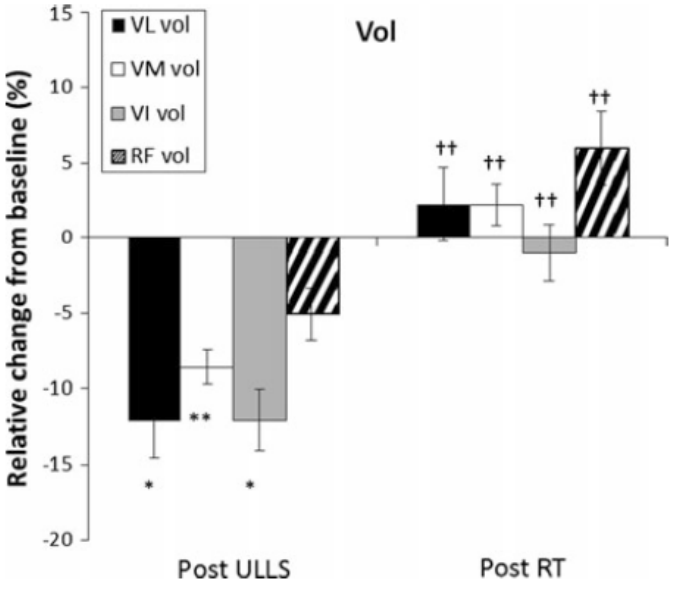

Figure 8.1

Fig. 8.2 a

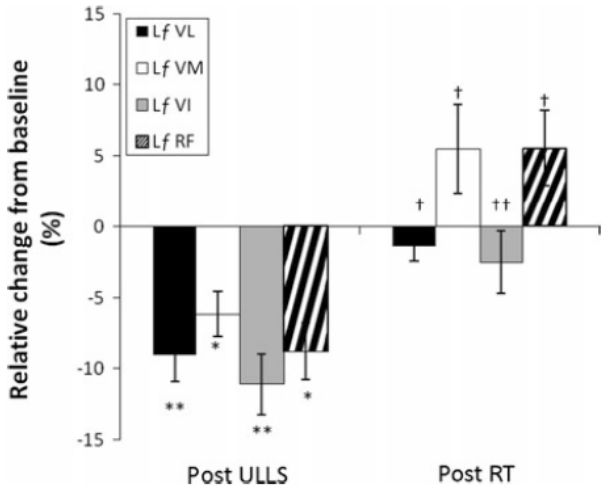

Fig. 8.2 b

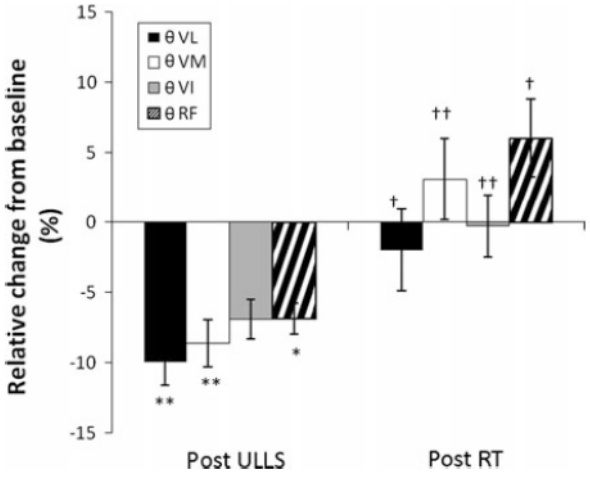

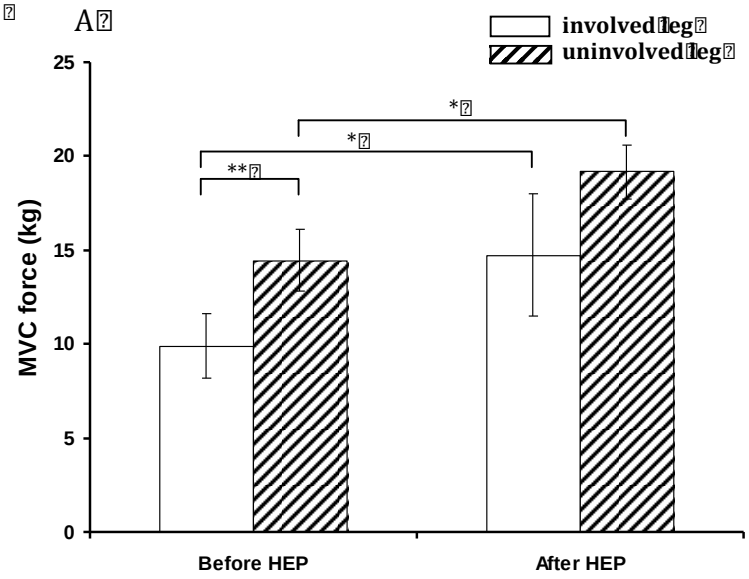

Figure 8.3

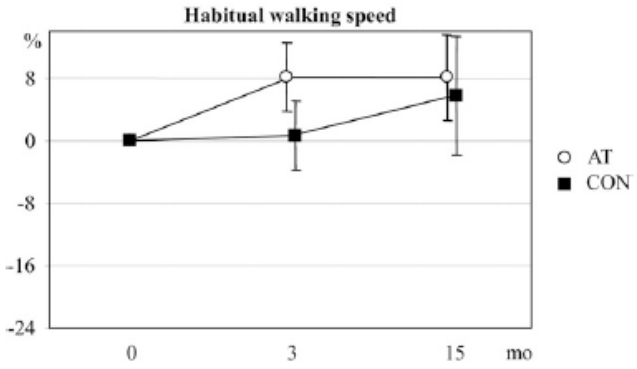

Figure. 8.4

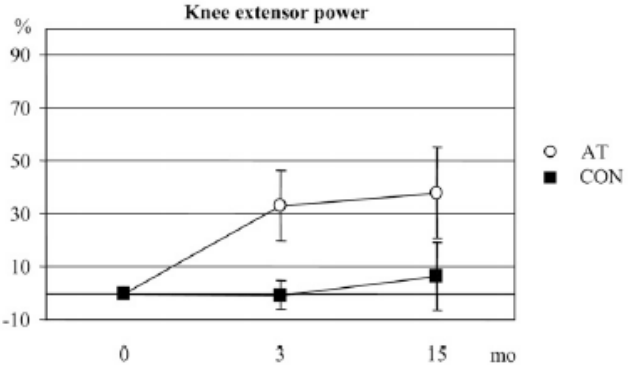

Figure.8.5

.

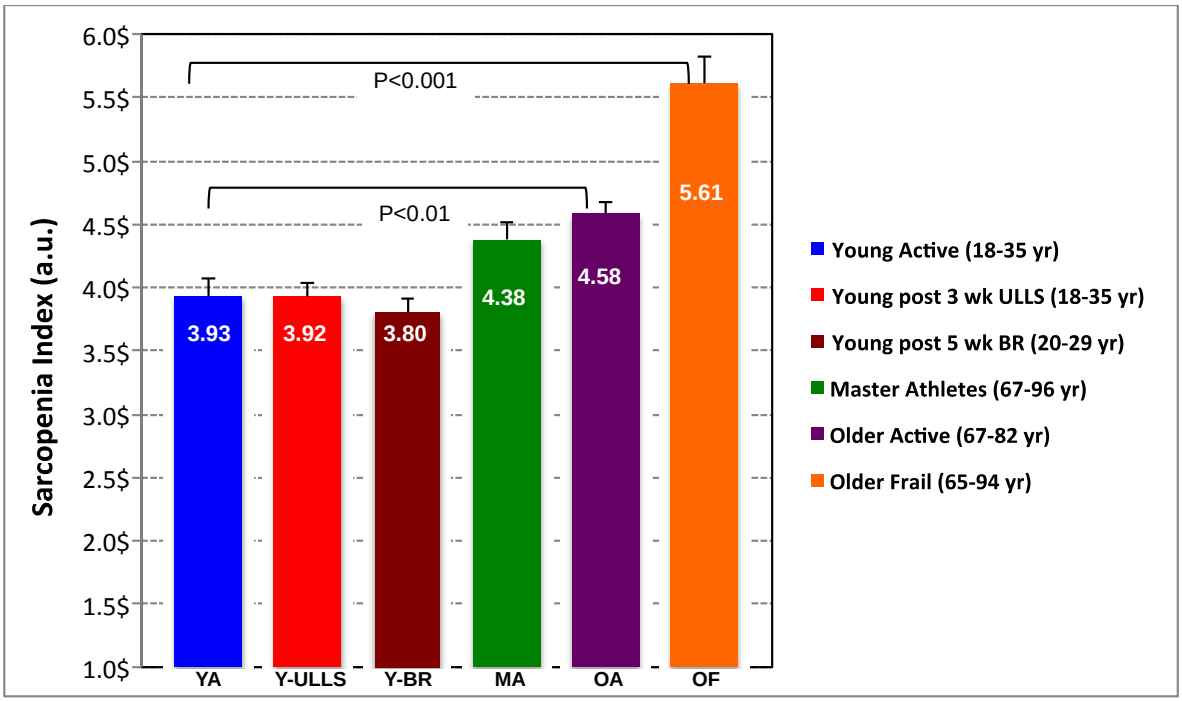

Figure 8.6

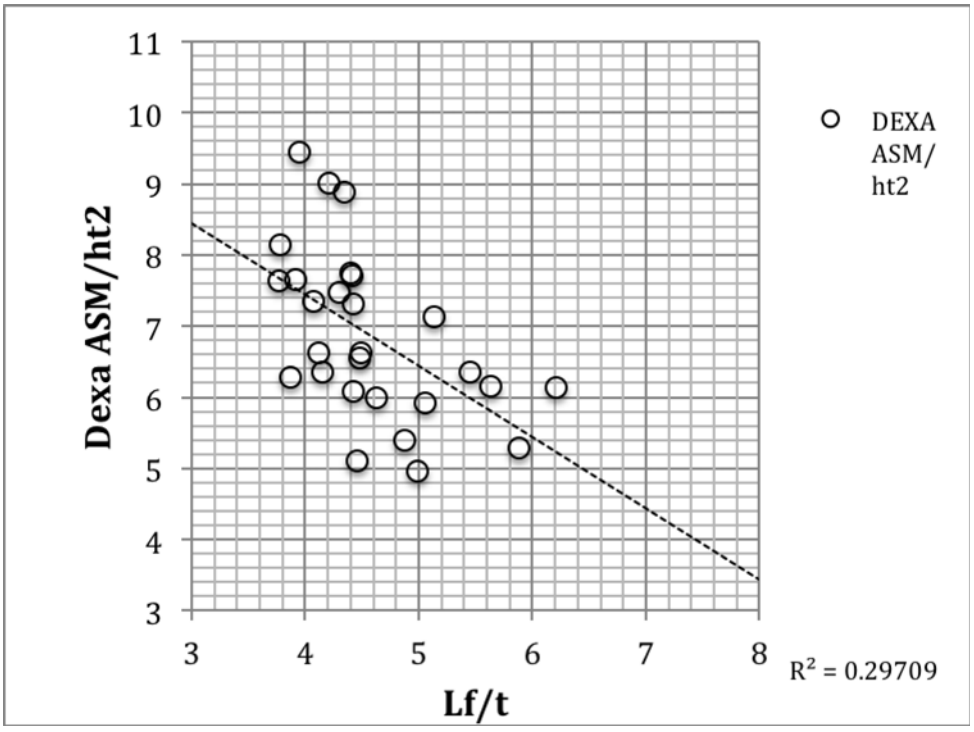

Figure 8.7

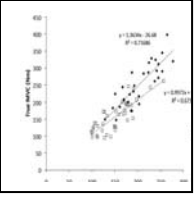

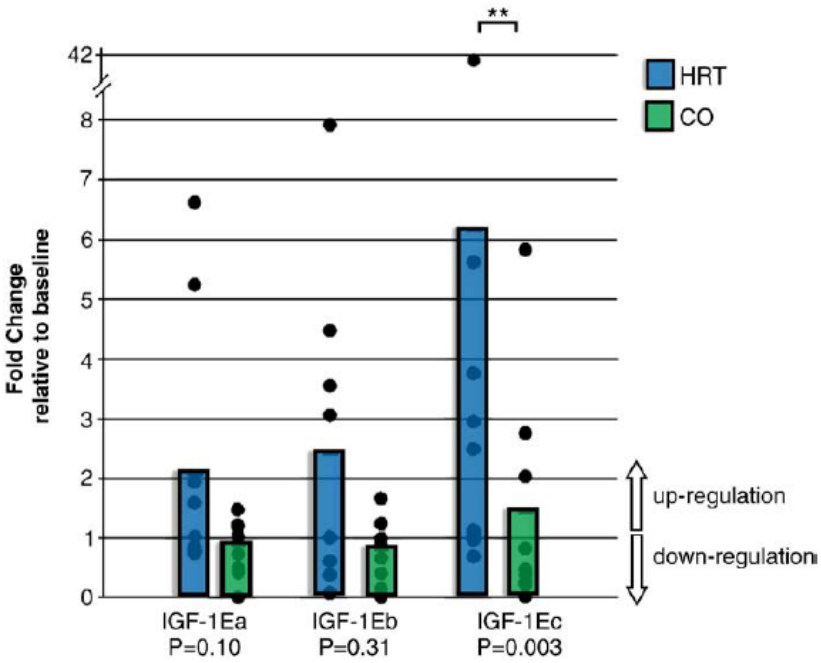

Figure 9.1 Change in the gene expression of IGF-1 splice variants in RCT HRT-study (*Pöllänen et al. 2010)*

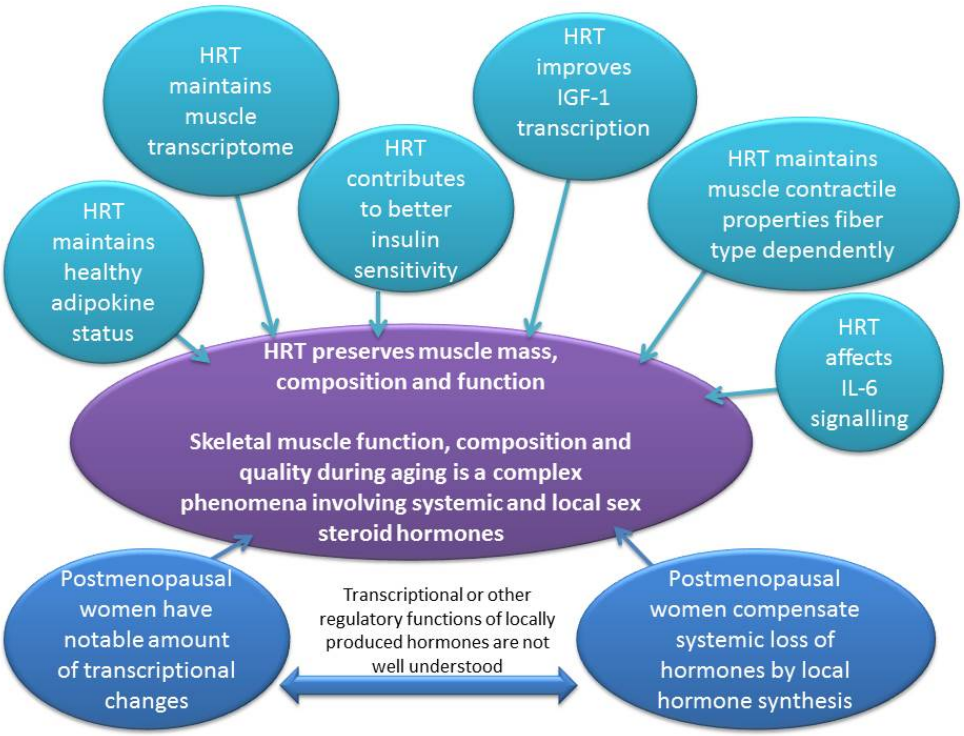

Figure 9.2 Contribution of HRT on skeletal muscle function, composition and quality in postmenopausal women.